

# Quantitative magnetic susceptibility mapping (QSM) in breast disease reveals additional information for MR-based characterization of carcinoma and calcification

F. Schweser<sup>1,2</sup>, K-H. Herrmann<sup>1</sup>, A. Deistung<sup>1</sup>, M. Atterbury<sup>1,3</sup>, P. A. Baltzer<sup>4</sup>, H. P. Burmeister<sup>4</sup>, W. A. Kaiser<sup>4</sup>, and J. R. Reichenbach<sup>1</sup>

<sup>1</sup>Medical Physics Group, Dept. of Diagnostic and Interventional Radiology 1, Jena University Hospital, Jena, Germany, <sup>2</sup>School of Medicine, Friedrich Schiller University of Jena, Jena, Germany, <sup>3</sup>Dept. of Physics, Brown University, Providence, RI, United States, <sup>4</sup>Dept. of Diagnostic and Interventional Radiology 1, Jena University Hospital, Jena, Germany

**INTRODUCTION** – During the last 20 years MR mammography (MRM) has proven to be a powerful and highly sensitive modality to detect and study breast cancer<sup>1</sup>. However, the diagnosis of breast carcinoma in early stage is still challenging. For example, MRM lacks clinical detectability of micro-calcifications, which are a hallmark sign for pre-invasive breast cancer. Recently, Fatemi-Ardekani et al.<sup>2</sup> demonstrated in an initial study that identification of micro-calcifications is possible using gradient echo (GRE) phase data due to the different magnetic properties of calcifications and glandular tissue. The observed phase contrast may in principle also be used as an input for quantitative magnetic susceptibility mapping (QSM), which is a novel technique for generating local quantitative anatomical tissue contrast<sup>3</sup>. In the current initial study, we demonstrate QSM in the breast. The preliminary results show that this novel quantitative contrast provides additional information about breast lesions potentially improving clinical diagnoses.

## MATERIALS & METHODS

**Data Acquisition:** Data were acquired during routine dynamic MRM examinations in five patients with invasive breast carcinoma using a 3D dual echo GRE sequence<sup>4</sup> ( $TE_1/TE_2/TR/FA/BW = 2.38\text{ ms}/4.76\text{ ms}/8.5\text{ ms}/20^\circ/435\text{ Hz/px}$ , matrix  $384 \times 384$ , voxel size  $0.91 \times 0.91 \times 3\text{ mm}^3$ , transverse orientation) on a 1.5T MR-scanner (Avanto, Siemens Medical Solutions). The total imaging time for one sequence run was 60s. After a native scan  $0.1\text{ mmol/kg}$  body weight Gd-DTPA (Omniscan, Schering AG, Berlin, Germany) was injected intravenously. 30s after contrast agent (CA) injection another seven scans were successively acquired.

**Data Processing:** Magnitude and phase images were reconstructed from the complex GRE data. The pre-CA phase images of the in-phase (IP) echo ( $TE=4.76\text{ ms}$ ) were pre-processed using the SHARP method<sup>5</sup>, and susceptibility maps were computed from the resulting images with an algorithm described by Schweser et al.<sup>6</sup>. Furthermore, standard IP magnitude subtraction images were calculated from the pre-CA and late CA (i.e., the 8<sup>th</sup> scan) magnitude data.

**RESULTS** – Figure 1 depicts representative slices of a patient (72y) after receiving breast-conserving therapy due to a pleomorphic carcinoma in the right breast. For this patient additional mammographic X-ray images were available, demonstrating various micro-calcifications (red arrows in Fig. 1g). A rapidly CA-enhancing structure was observed surrounding a potential lipoid necrosis in the subtraction images (Fig. 1c; blue arrow). The contrast of the IP magnitude and phase images (Fig. 1a,b) is rather unspecific. The susceptibility map (Fig. 1e) reveals positive contrast for the structure visible in the CA-enhanced images (blue arrows in Fig. 1c,e). Furthermore, diamagnetic calcifications are visible as negative contrast (red arrows in Fig. 1e). The minimum intensity projection (mIP) of the susceptibility map (Fig. 1f) reveals delineation of numerous calcifications with clustering close to the pectoralis muscle. Figure 2 shows representative slices of a patient (74y) with an invasive polylobular carcinoma in the right breast. A rapidly enhancing structure is visible in the CA-enhanced magnitude subtraction images (Fig. 2a,c). The overall contrast of the susceptibility maps (Fig. 2b,d) is, again, similar to these images, delineating the breast lesion as well as Cooper's ligaments and feeding vessels. The overall shape of the enhancing lesion is, however, larger (red outline and red arrows in Fig. 2) than in the CA-enhanced images and shows deviating contrast in some regions (green arrows in Fig. 2).

**DISCUSSION & CONCLUSIONS** – This initial study demonstrated, for the first time, that clinical application of QSM in the breast is feasible. QSM has been shown to enable unambiguous identification of calcifications (Fig. 1f), which appear hypo-intense due to their diamagnetic susceptibility. Identification of calcifications is of tremendous importance, since X-ray mammography in regions close to the pectoralis muscle is difficult and calcifications in these regions may remain unidentified with conventional X-ray imaging techniques (cf. Figs. 1f and 1g). The computed susceptibility maps were obtained without CA and provided contrast similar to the CA-enhanced magnitude difference images, though with increased sharpness of the lesion boundaries (cf. Figs. 2a and 2b). QSM may, thus, be taken as an alternative contrast in MRM to yield additional information about tumor morphology and vascularization.

Furthermore, the proposed method is of particular interest for patients with renal insufficiency or nephrogenic systemic fibrosis (NSF), a contra-indication of contrast agent injection. It has to be noted that in the current study a standard clinical GRE sequence with a short TE had been used to acquire the data. Thus, optimization of the sequence for QSM is likely to result in highly improved image quality compared to the maps presented here. For instance, more isotropic voxels may be acquired and the signal to noise ratio may be improved by increasing the echo time, e.g., to multiples of the IP time. Although the origin of the observed hyperintense susceptibility contrast is not yet fully understood, it may be assumed that it is related to the high density of vessels and the increased oxygen extraction fraction<sup>7</sup> in these regions. Future research will focus on investigating the sources of this contrast and on clinical studies to examine whether QSM provides a benefit for clinical diagnoses.

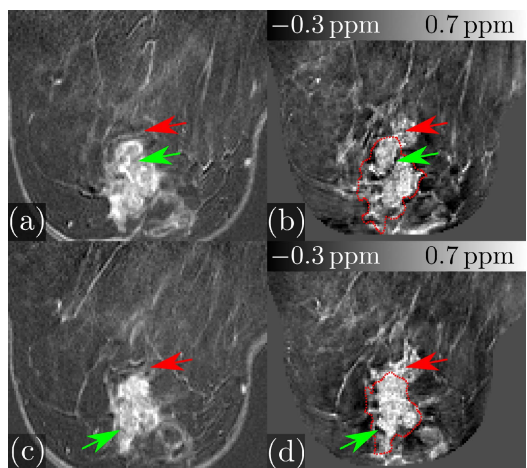


**FIGURE 2.** Representative slices of the contrast enhanced magnitude subtraction images (left column) and corresponding susceptibility maps computed from the pre-CA phase data (right column). The red outline in (b and d) indicates the enhancing region in the magnitude subtraction images (a and c).

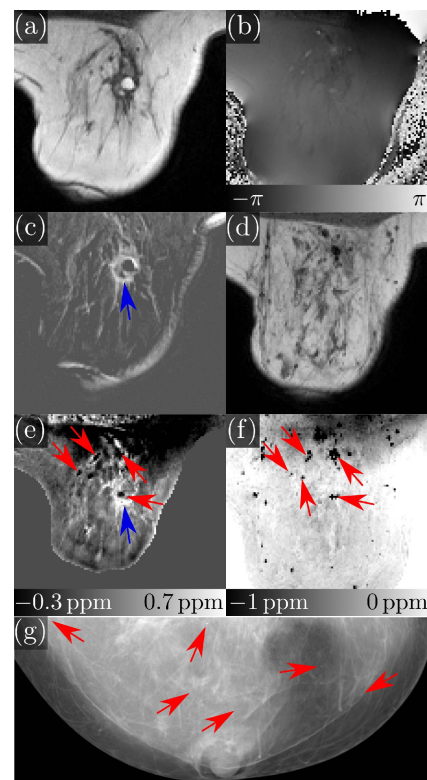


**FIGURE 1.** Representative slices of pre-CA magnitude (a) and raw phase (b) data, contrast enhanced magnitude subtraction image (c), susceptibility map (e), and a craniocaudal X-ray image (g). A minimum intensity projection of the late-CA magnitude images and the susceptibility map are shown in (d) and (f), respectively. Note, red arrows in (e,f) and (g) do not necessarily mark the same calcifications.

**REFERENCES** – [1] Kaiser WA and Zeitler E. *Radiology*. 1989;170(3):681-6. [2] Fatemi-Ardekani A, et al. *Med Phys*. 2009;36(12):5429-36. [3] Li L. *Magn Reson Med*. 2001;46(5):907-16. [4] Herrmann, K-H, et al. *ISMRM*. 2009, p. 4130. [5] Schweser et al. *NeuroImage*. 2010. [6] Schweser et al. *Med Phys*. 2010;37(9):5165-78. [7] He X and Yablonskiy DA. *Magn Reson Med*. 2007;57(1):115-26.